Optically optimized transmittive and reflective bistable twisted nematic liquid crystal displays

S. T. Tang, H. W. Chiu, and H. S. Kwok[a)]
Center for Display Research, Hong Kong University of Science and Technology, Clear Water Bay, Hong Kong

(Received 20 July 1999; accepted for publication 7 October 1999)

A new Mueller matrix approach is developed for the design of optical modes for all nematic liquid crystal displays (LCD). In particular, for linearly polarized light going into the LC cell, conditions for linear polarization and circular polarization outputs are obtained. By considering the switching between different polarization modes, new transmittive and reflective bistable twisted nematic (BTN) LCD operating conditions with optimized contrast and brightness are discovered. A passive matrix driven single polarizer reflective BTN display was fabricated with reasonably good measured optical performance and fast selection time. © *2000 American Institute of Physics.* [S0021-8979(00)00602-2]

I. INTRODUCTION

Bistable twisted nematic (BTN) displays that switched between two metastable twisted nematic states electrically were first discovered by Berremen and Heffner in 1981.[1] The two bistable twist angles were 0 and 2π. In 1995, a high quality passive matrix driven BTN display with a large number of scanning lines was realized by Tanaka *et al.*[2] Since then, the BTN display has attracted great attention and several detailed studies on the bistable mechanism have been reported.[3] These BTN LCDs are attractive because of two main reasons: (1) Since both metastable twist states of the BTN display have in-plane alignment, the viewing angle is very large. (2) Because of the inherent memory effect, a BTN display can be multiplex driven with good image quality and without crosstalk.

While most people have concentrated on the $(0, 2\pi)$ system, we have proposed and demonstrated the $(-\pi/2, 3\pi/2)$ and $(\pi/2, 5\pi/2)$ transmittive BTNs,[4] as well as the $(-36°, 324°)$ reflective BTN with a single polarizer.[5] However, it is now realized that all of the BTN optical modes that have been studied so far, including the $(0, 2\pi)$ system, are not quite well optimized in terms of their optical properties. It is the purpose of this article to point out a proper way to optimize the optical brightness and contrast ratio of a BTN, both in transmission and in reflection.

The optical properties of a BTN cell is characterized by four parameters, namely, the twist angle (ϕ), the retardation ($d\Delta n$), the input polarizer angle (α), (relative to the input LC director), and the output polarizer angle (γ). For the case of a single polarizer reflective BTN display, the parameter γ is not necessary and there are only three parameters. The twist angles of the two metastable states always differ by 2π. The operating conditions of these BTN modes in Refs. 4 and 5 were obtained using the 2D parameter space technique.[6] However, because of the multitude of free parameters in the BTN, the 2D parameter space in fact cannot produce all the optimized optical modes. One obvious drawback is the assumption that the input–output polarizers are either perpendicular or parallel to each other. In this article, we shall show that by using the 4×4 Mueller matrix,[7,8] this assumption is not necessary. Many new optical modes for the BTN can be discovered with good optical properties. Experimental verification will also be presented for the case of a single polarizer reflective display. This reflective BTN can be passive matrix driven with good contrast and brightness. The selection time was 600 μs.

Recently, Suh *et al.* studied the propagation of the Stokes parameter in a general TN cell.[9] By using a Stokes parameter and Poincare sphere approach, they have successfully derived the results for linear and circular outputs of a linear polarization input. However the results are restricted to the case of input polarizer parallel to the input director. Likewise, in a recent paper, Kim *et al.* analyzed the reflective BTN using the Mueller matrix approach, but again with the restriction of zero polarizer angles.[10] In this article we will show that if all four parameters are allowed to vary independently, a complete set of BTN modes can be obtained.

II. CONDITIONS FOR OPTICALLY OPTIMIZED BTN DISPLAYS

Here we will introduce the concept of polarization transformation. For a linear polarization input to a twisted nematic cell, in general, the output polarization would be elliptical. However under certain specific combinations of cell parameters, the output polarization can be either linearly or circularly polarized. They shall be referred to as the LP and CP conditions, respectively. It turns out that for any input polarization angle α, there are, in general two LP conditions and one CP condition.

A. Transmittive BTN displays

A BTN display has two metastable twisted nematic states. Assuming ideal polarizers, an optically optimized transmittive BTN should have unity transmittance in one

a)Electronic mail: eekwok@ust.hk.

state and zero transmittance in the other state. Thus the two metastable states should possess the following properties. (1) The switching is between two LP states, labeled LP1 and LP2 states. (2) The retardations ($d\Delta n$) of both states are the same, so that it is essentially the same LC cell. (3) The twist angles of the LP1 and LP2 states should differ by 2π. Then they will correspond to the two bistable twist states. (4) The output linear polarization angle of the LP1 and LP2 states should be perpendicular to each other ($\gamma_1-\gamma_2=\pm 90°$).

B. Reflective BTN display

Reflective BTNs are here defined as the true reflective displays with only one front polarizer and a rear reflector is attached directly to the glass.[11] The rear polarizer is eliminated leading to a potentially brighter display with no viewing parallax.[12] The required conditions for optically optimized reflective BTNs are: (1) The switching is between a LP state and a CP state; (2) the retardation ($d\Delta n$) of both states is the same; (3) the twist angles of the bistable states differ by 2π.

For RBTN, condition (4) of the BTN case is automatically fulfilled. By passing through the LC cell twice, under the CP condition, the output polarization is orthogonal to the input polarization. The equations that govern the polarization transformations will now be derived next.

III. LP AND CP TRANSFORMATIONS: MUELLER MATRIX

In order to study the polarization transformation effect of a twisted nematic cell, a Mueller matrix that represents a general twisted nematic cell was derived from its Jones matrix analog.[7]

The Mueller matrix **M** has the form,

$$M=\begin{pmatrix} 1 & 0 & 0 & 0 \\ 0 & a^2+b^2-c^2-d^2 & 2(bd-ac) & -2(ad+bc) \\ 0 & 2(ac+bd) & a^2-b^2-c^2+d^2 & 2(ab-cd) \\ 0 & 2(ad-bc) & -2(ab+cd) & a^2-b^2+c^2-d^2 \end{pmatrix}$$

where

$$a=\cos\phi\cos\chi+\frac{\phi}{\chi}\sin\phi\sin\chi$$

$$b=\frac{\delta}{\chi}\cos\phi\sin\chi$$

$$c=\sin\phi\cos\chi-\frac{\phi}{\chi}\cos\phi\sin\chi$$

$$d=\frac{\delta}{\chi}\sin\phi\sin\chi$$

with $\delta=\pi d\Delta n/\lambda$ and $\chi^2=\delta^2+\phi^2$. Here d is the cell gap thickness, Δn is the birefringence of the LC material, ϕ is the twist angle, and λ is the wavelength of incident light.

It is convenient to write the Mueller matrix in the form:

$$M=\begin{pmatrix} 1 & 0 & 0 & 0 \\ 0 & A & B & C \\ 0 & D & E & F \\ 0 & G & H & K \end{pmatrix}.$$

The resultant Stokes vector for a linear incident light at angle α is obtained by $\mathbf{S'=M*S}$ which written explicitly is

$$S=\begin{pmatrix} 1 & 0 & 0 & 0 \\ 0 & A & B & C \\ 0 & D & E & F \\ 0 & G & H & K \end{pmatrix}\begin{pmatrix} 1 \\ \cos 2\alpha \\ \sin 2\alpha \\ 0 \end{pmatrix}.$$

For a linear polarization output, we shall have $\mathbf{S'}=(1\ \cos 2\gamma \sin 2\gamma\ 0)^T$ for some angle γ. Thus we have $G\cos 2\alpha+H\sin 2\alpha=0$. There are two solutions for this equation. They are labeled the LP1 and LP2 solutions:

LP1

$$\delta^2+\phi^2=(N\pi)^2, \tag{1a}$$

$$\gamma=\phi+\alpha, \tag{1b}$$

LP2

$$\frac{\phi}{\sqrt{\delta^2+\phi^2}}\tan\sqrt{\delta^2+\phi^2}=\tan 2\alpha, \tag{2a}$$

$$\gamma=\phi-\alpha. \tag{2b}$$

The physical meaning of the LP1 and LP2 solutions can be understood if we examine the Mueller matrix **M**. When Eq. (1a) is substituted into the Mueller matrix **M**, it takes on the form of a polarization rotation matrix of angle ϕ. Thus the output polarizer angle $\gamma=\phi+\alpha$ as indicated in Eq. (1b) is just the result of such a polarization rotation. Indeed, the LP1 modes are very similar to the regular Mauguin modes or the waveguiding modes of a general TN LCD[6]. In these modes, the effect of the twisted LC structure is simply to rotate the polarization of the incoming light by the twist angle.

When Eq. (2a) is substituted into M, it takes on a form which is the combination of a retardation plate and a polarization rotator. The output polarizer angle can be obtained to be $\gamma=\phi-\alpha$, which is consistent with Eq. (2b). The physical

TABLE I. The first six transmittive BTN solutions by solving Eqs. (5) and (1b). The $d\Delta n$ values are calculated with $\lambda = 0.55$ μm.

$d\Delta n/\mu$m	ϕ_1	ϕ_2	γ
0.273*	−348.75	11.25	−33.75
0.3994*	−123.75	236.25	−78.75
0.522*	56.25	416.25	101.25
0.733	−483.75	−123.75	11.25
0.765*	−258.75	101.25	56.25
0.932	191.25	551.25	56.25

meaning of the LP2 mode is therefore that of a polarization rotator and a half-wave plate which reflects the polarization angle by 2α.

In order to calculate the circular polarization (CP) output condition, the equation $\mathbf{S}'=\mathbf{M}^*\mathbf{S}$ is rearranged. Since $\mathbf{M}$ is unitary, one can write $\mathbf{M}^{\mathbf{T}}\mathbf{S}'=\mathbf{S}$ where $\mathbf{M}^{\mathbf{T}}$ is the transpose of $\mathbf{M}$. Because a circular output means $\mathbf{S}'=(100\pm 1)^T$, therefore we have the conditions $K=0$ and $\tan 2\alpha = H/G$ for circularly polarized light output.

The solution of these two equations is given by CP

$$\frac{\delta^2}{\delta^2+\phi^2}\sin^2\sqrt{\delta^2+\phi^2}=\frac{1}{2}, \tag{3a}$$

$$\tan 2\alpha = \frac{-\sqrt{\delta^2+\phi^2}}{\phi}\cot\sqrt{\delta^2+\phi^2}. \tag{3b}$$

For each given input polarizer angle therefore, there is a specific set of values (δ, ϕ) that will give the CP condition. In general, there are an infinite number of possibilities.

IV. TRANSMITTIVE BTN

Now we have enough tools for BTN/RBTN optical mode design. According to the conditions listed in Sec. II A a transmittive BTN is limited to be:

(1) A switching between different LP types, that should be an LP1–LP2 switching because, if they are of the same LP type, condition (4) of orthogonal output cannot be fulfilled.

(2) The input polarizer angle α should be equal to $\pm 45°$.

For an input polarizer angle α of 45°, the LP2 solution is reduced to

$$\delta^2+\phi^2=(M-\tfrac{1}{2})^2\pi^2, \tag{4}$$

where M is a positive integer. Because the retardation δ will remain unchanged and the twist angles differ by 2π, eliminating δ in Eqs. (1a) and (4), we arrive at the following equation:

$$\phi_1=\frac{[(M-0.5)^2-N^2-4]\pi}{4}, \tag{5}$$

where ϕ_1 is the twist angle of the LP1 mode and M, N are positive integers. The first six solutions of Eq. (5) are listed in Table I.

The input polarizer angle α value is fixed at 45°. The output polarizer angle γ has two choices, one is to optimize the bright state overall luminance, while the other, which is orthogonal to the first one, will give an optimized contrast. The γ values given in Table I are assigned so that maximum overall contrasts are obtained. Notice that in Table I, if all the angles are reversed in sign, we should get the same mode. Thus, the first mode (−348.75°, 11.25°) is the same as a (−11.25°, 348.75°) BTN. Similarly, the fifth BTN mode in Table I (−258.75°, 101.25°) is the same as a (−101.25°, 258.75°) BTN. Comparing the $d\Delta n$ values as well, these two modes are similar to the (0, 2π) and ($-\pi/2$, $3\pi/2$) BTN previously studied.[5]

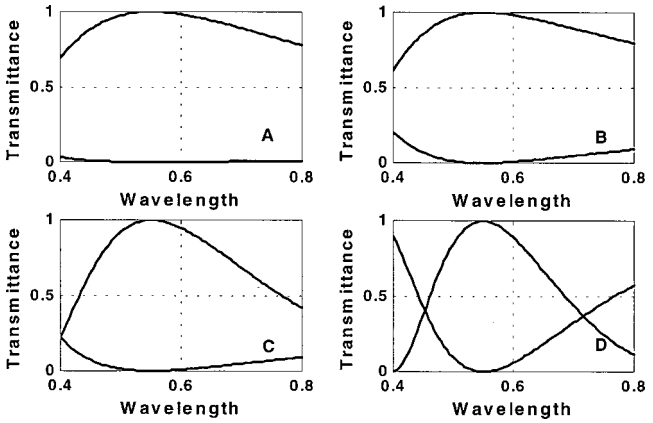

FIG. 1. Transmission spectra of selected BTN modes. Plots $A-D$ are modes with $d\Delta n = 0.273$, 0.3995, 0.523, and 0.765 μm, respectively.

The above analysis guarantees only a good mode at a particular wavelength (550 nm). Further considerations have to be made on the dispersion characteristic and the stability of higher twist (>450°) states. For this reason, higher twist states are not listed in Table I, as bistability is difficult to obtain in those cases. Four good optical modes (with asterisk in Table I) are chosen to be examined further. Figure 1 shows the transmission against wavelength plots of these chosen modes. Plots $A-D$ (solid lines) are the BTNs with $d\Delta n = 0.273$, 0.3995, 0.523, and 0.765 μm, respectively. It can be seen that the dispersion characteristics of the first three modes are excellent. For the (−11.25°, 348.75°) BTN (curve *A*), the spectra are comparable to the waveguiding TN mode display. There is almost no wavelength dependence in the transmission. Cases *B*, *C*, and *D* show progressively more dispersion.

The parameters for cases *A* and *D* are very similar to those of the (0, 2π) and ($-\pi/2$, $3\pi/2$), respectively. Comparing curves *A* and *D* with the published spectra, it can be seen that the present results are better in terms of the overall contrast and the wavelength independence. Plots *B* and *C* are completely new.

V. REFLECTIVE BTNs

The operation of a RBTN display be viewed as a switching between LP states and CP states, where the LP states are the bright state while the CP states are the dark states. (The dark and bright state can be reversed if a polarizing beam splitter is used instead of a sheet type polarizer.)

TABLE II. Reflective BTN modes (LP1-CP switching).

$d\Delta n/\mu$m	ϕ_1	ϕ_2	α
0.1369	−2.8	362.8	43.22
0.4020*	−24.9	335.1	−39.53
0.5932	143.9	503.9	−21.09
0.6612*	−72.3	287.7	35.26
0.8518	−132.2	227.8	−30.86
0.9148	89.4	449.4	36.32

Since we have two LP solutions, the RBTN optical modes can be divided into two groups.

Group 1: LP1–CP switching

Let the twist angle of the CP solution be ϕ_1 and that of LP1 be $\phi_2=\phi_1+2\pi$, then by eliminating δ from Eqs. (1a) and (3a), Eq. (6) is obtained:

$$\frac{(N\pi)^2-(\phi_1+2\pi)^2}{(N^2-4)\pi^2-4\pi\phi_1}\sin^2\sqrt{(N^2-4)\pi^2-4\pi\phi_1}=0.5. \tag{6}$$

The first group of solutions for $N=2$ and 3 with $d\Delta n$ less than 1 μm are listed in Table II. The input polarizer angle α is calculated from Eq. (3b).

Group 2: LP2–CP

Again, by solving Eqs. (2a), (3a), and (3b) simultaneously, the second group of solutions can be found. The reflectance versus wavelength plots of some chosen RBTN modes (with asterisks in Table II and III) are given in Fig. 2. Curves $A-D$ (solid lines) are the RBTNs with $d\Delta n=0.4$, 0.66, 0.31, and 0.37 μm, respectively.

In the literature, only one RBTN has been reported previously by Xie *et al.*[5] with bistable twist angles of −36° and 324°. This RBTN mode was obtained by searching the Jones matrix parameter space. Indeed it is a very good mode with large retardation value ($d\Delta n=0.94\,\mu$m). This mode is not obtained directly from the present approach because it is not an exact solution of the equations above. It is actually quite siimilar to the last mode in Table III. All the RBTN modes reported here are exact. They are new and have not been reported before.

VI. EXPERIMENTAL RESULTS: RBTN DISPLAY

Using the above calculated results, a dot matrix single polarizer reflective BTN display was fabricated. The cell parameters chosen were $d\Delta n=0.4\,\mu$m, $\phi=-25°$, $\alpha=-40°$. The d/P ratio was varied carefully in order to obtain bistability. According to the heuristic argument, the d/P ratio should favor the $\phi+\pi$ state in order to obtain bistability. This corresponds to 0.43. Experimentally, we found that bistability could be obtained for d/P from 0.5 to 0.55. This is consistent with the observations in Ref. 4 that the optimal d/P is always larger than the heuristic d/P ratio of $(\phi+\pi)/2\pi$.

TABLE III. Reflective BTN modes (LP2-CP switching) with $d\Delta n$ less than 1 μm.

$d\Delta n/\mu$m	ϕ_1	ϕ_2	α
0.3108*	−67.2	292.8	−24.24
0.3676*	49.3	409.3	32.85
0.678	42.5	402.5	−39.5
0.737	−176	184	−21.38
0.745	174	534	22.14
0.955	−31	329	−42.09

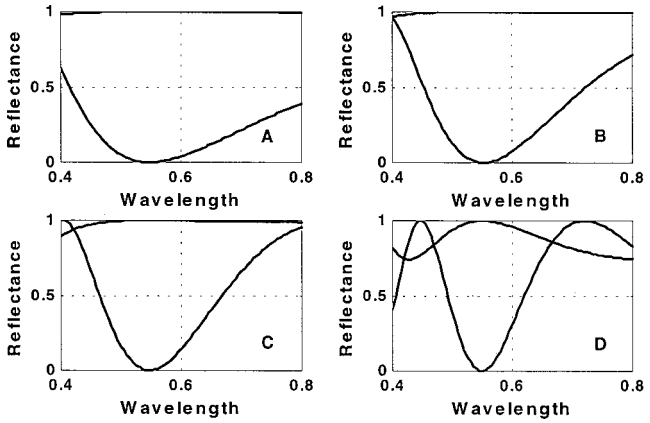

FIG. 2. Reflectance spectra of selected RBTN modes with $d\Delta n=0.31$, 0.37, 0.4, and 0.66 μm, respectively. Notice that the on-state for the upper two curves is very close to the $R=1$ axis and cannot be seen clearly.

The contrast ratio was measured by using a polarizing beam splitter (PBS). Employing a He–Ne laser at 632.8 nm as the light source, the contrast ratio was found to be 100:1. The full reflection spectrum of the RBTN was measured by using a fiber optics reflection probe with a tungsten halogen light source, and a PR650 spectrophotometer. In this experiment, a sheet polarizer was used instead of a PBS. The experimental and calculated results are shown in Fig. 3.

It can be seen that the agreement between theory and experiment is rather good. The shapes of the curves are the same. However, they differ in the magnitudes of the maxima and the minima. That difference can be accounted for by the liquid crystal dispersion. In the shorter wavelength region, the birefringence Δn of the LC is larger. Thus the reflectance curve shifts to the right. The design parameter of 0.4 μm for $d\Delta n$ was fulfilled only at about 590 nm. This fact is confirmed if one notices that the minimum points for in both the

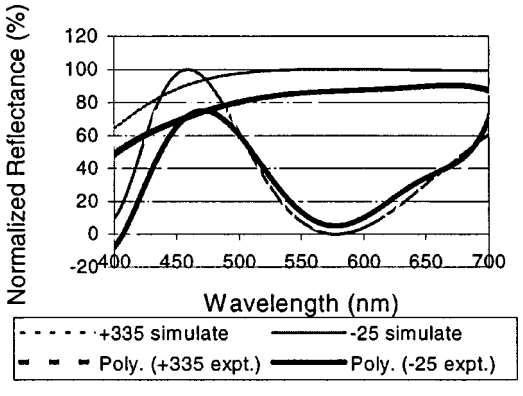

FIG. 3. Theoretical and experimental reflectance vs wavelength curves.

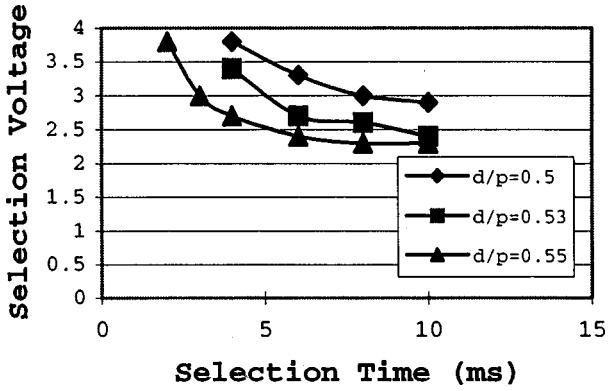

FIG. 4. Selection voltage vs selection time for different d/P ratios.

simulation and measured curved were not exactly at 550 nm, but a bit shifted to the longer wavelength side. Moreover, there is strong surface reflection from the RBTN so that the dark state cannot reach $R=0$. Hence the contrast is not as high as predicted.

In order to minimize the reset voltage, the select voltage and the reset time, a series of experiments with different d/P ratio were carried out. The results are shown in Figs. 4 and 5. In Fig. 4, there is a clear trend of larger selection time leading to smaller selection voltage. Also the decrease of selection voltage becomes saturate when the selection time reaches about 10 ms. The reset voltage in Fig. 4 was 20 V and the reset time was 25 ms. In Fig. 5, the reset voltage was plotted against the reset time for different d/P ratios. It is seen that larger reset time leads to smaller reset voltage. The decrease of reset voltage becomes saturated when the reset time reaches 150 ms. The selection voltage in Fig. 5 was 4 V and the selection time was 4 ms. From these results, it is clear that the voltage applied and its duration cannot be decreased at the same time. The actual voltage applied and its duration should be chosen according to the particular application.

The reset voltage was then fixed at 40 V for 20 ms and then a time delay was introduced before the start of the selection voltage.[13] The selection time was drastically reduced to 600 μs. This makes faster driving possible. The experiment results are summarized in Fig. 6.

Figure 7 shows a photograph of the RBTN sample fabricated. It is passive-matrix driven to display a Chinese character in a 32×32 matrix. Finally, it should be pointed out that the BTN is not truly bistable. The ϕ and $\phi+2\pi$ states are forced upon the LC cell by the boundary conditions (rubbing conditions of the alignment layers). However, as can be seen above, the d/P ratio actually favors the $\phi+\pi$ twist state. So in practice, the ϕ and $\phi+2\pi$ states will relax back to the more stable $\phi+\pi$ state slowly. Experimentally, it was observed that the relaxation time was about several seconds for the samples we fabricated. So the BTN is not as bistable as the bistable cholesteric display. It may limit its application somewhat in practice.

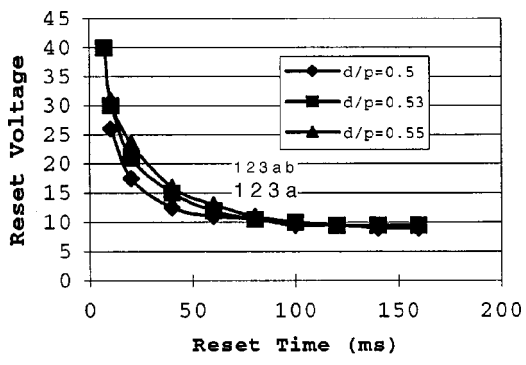

FIG. 5. Reset voltage vs reset time for different d/P ratios.

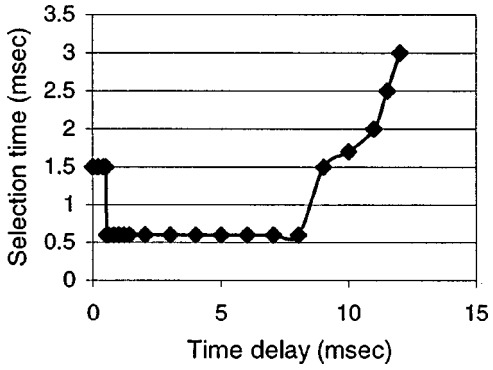

FIG. 6. Selection time vs time delay.

VII. CONCLUSIONS

In this article, we have introduced the concept of polarization conversion for a general twisted nematic LC cell. Conditions for linear polarization and circular polarization output are obtained using the Mueller matrix. By applying this polarization analysis to the case of BTN, we have successfully derived the equations that relate the cell parameters of optically optimized BTN and RBTN displays. By solving these equations, operating conditions for all BTN and RBTN with excellent optical properties are obtained. These modes have excellent contrast and brightness because the condition for their optimization is $T=1$ for one twist state and $T=0$ for the other twist state. Therefore, they must have infinite contrast and maximum brightness at one wavelength.

We demonstrated a RBTN dot matrix display using one of the parameters obtained. It was driven with passive ad-

FIG. 7. A 32×32 dot matrix RBTN display prototype. It is a single polarizer reflective type display without backlight.

dressing. The experimentally obtained contrast, spectra, and brightness are similar to the predictions. However, the contrast is not as good, mostly because of surface reflection of the RBTN. Nevertheless, the value of 100:1 obtained is quite good. We also studied the minimization of the selection voltage, the selection time, the reset voltage, and the reset time as a function of the d/P ratio. A 600 μs selection time was achieved.

Further enhancement of the BTN/RBTN displays could be carried out in two aspects. First, the ultimate optically optimized display should include the effect of LC birefringence dispersion, as well as the actual nonideal optical properties of the polarizer and the light source. Second, the stable $\phi+\pi$ state should be eliminated so that the BTN can truly be bistable. Otherwise the ϕ and $\phi+2\pi$ states will decay too rapidly. Also, the driving scheme may need some improvement in order to make it compatible to conventional STN drivers for commercialization.

ACKNOWLEDGMENT

This research was supported by a grant from the Hong Kong Industry Department.

[1] D. W. Berremen and W. R. Heffer, J. Appl. Phys. **52**, 3032 (1981).
[2] T. Tanaka, Y. Sato, A. Inoue, Y. Momose, H. Nomura, and S. Iino, IDRC (Asia Display, 1995), p. 259.
[3] T. Z. Qian, Z. L. Xie, H. S. Kwok, and P. Sheng, Appl. Phys. Lett. **71**, 632 (1997).
[4] Z. L. Xie and H. S. Kwok, J. Appl. Phys. **84**, 77 (1998).
[5] Z. L. Xie and H. S. Kwok, Jpn. J. Appl. Phys., Part 1 **37**, 2572 (1998).
[6] H. S. Kwok, J. Appl. Phys. **80**, 3687 (1996).
[7] S. T. Tang and H. S. Kwok, Soc. Info. Disp. Symp. Dig. 552 (1998).
[8] S. T. Tang and H. S. Kwok, Soc. Info. Disp. Symp. Dig. 195 (1999).
[9] S. W. Suh, Z. Zhuang, and J. Patel, Soc. Info. Disp. Symp. Dig. 997 (1998).
[10] Y. J. Yim, Z. Zhuang, and J. Patel, Soc. Info. Disp. Symp. Dig. 866 (1999).
[11] F. H. Yu, J. Chen, S. T. Tang, and H. S. Kwok, J. Appl. Phys. **82**, 5287 (1997).
[12] J. Chen, F. H. Fu, H. C. Huang, and H. S. Kwok, Jpn. J. Appl. Phys., Part 1 **37**, 217 (1998).
[13] T. Tanaka, T. Obikawa, Y. Sato, H. Nomura, and S. Iino, IDRC (Asia Display, 1998), pp. 295–298.